

Investigating 2,5 Dihydroxybenzoic Acid as an Effective Matrix for ME-SIMS

A thesis submitted in partial fulfillment of the requirement
for the degree of Bachelor of Science with Honors in
Physics from the College of William and Mary in Virginia,

by

Laurel Averett

Accepted for _____
Honors

Advisor: Dr. William Cooke

Dr. Chris Carone

Dr. Brian Holloway

Dr. Todd Averett

Williamsburg, Virginia
May 2005

Acknowledgements

I would first like to thank my advisor Dr. Bill Cooke for his support and guidance. I would also like to thank Amy Wilkerson, Olga Trofimova, Dee Dee Hopkins, and Natalie Percy for their assistance with the instruments at the Applied Research Center. Finally, I would like to thank Dr. Brian Holloway, Dr. Todd Averett, and Dr. Chris Carone for their participation in my Honors Committee.

Contents

Abstract	ii
1 Introduction	1
2 Underlying Physics	4
2.1 Ionization	5
2.2 Molecular Liftoff	6
2.3 Volume of Ablated Material	7
2.4 Atomic Force Microscopy	8
3 Crystal Growth and Surface Analysis	9
4 Results	15
5 Discussion	19
6 Conclusions	27

Abstract

Matrix Enhanced Secondary Ion Mass Spectrometry (ME-SIMS) is a potential technique for analyzing large biomolecules. ME-SIMS uses sample preparation techniques common to matrix assisted laser desorption ionization (MALDI) to aid molecular liftoff without fragmentation in time of flight secondary ion mass spectrometry (ToF-SIMS). These preparation techniques involve dissolving the material to be studied in a solution of a matrix acid and an appropriate solute, then letting the solution dry on a sample substrate, forming crystals. The 2,5 dihydroxybenzoic acid (2,5 DHB) matrix is effective in MALDI, and has shown potential as an effective matrix in ME-SIMS. Matrix crystals were studied in the atomic force microscope (AFM) for surface structure, then were inserted and run in the ToF-SIMS instrument. The changes in surface structure due to the SIMS primary ion beam will predict the ability of ME-SIMS to analyze large biomolecules.

1 Introduction

Time of flight secondary ion mass spectrometry (ToF-SIMS) is a well developed method of surface analysis. In SIMS energetic ions bombard the surface of a sample, ejecting particles which are then detected by a ToF analyzer, as shown in Figure 1. It is effective for detecting small molecules on surfaces with parts per million or parts per billion sensitivity which makes it ideal for biological applications [1]. Also, the focusing capabilities of the primary ion beam in ToF-SIMS allows it to image with lateral resolution in the submicron range [2]. ToF-SIMS is a very successful surface characterization tool because it only analyzes the top few monolayers ($\sim 10 \text{ \AA}$) [3]. However, biomolecules are massive, fragile and often fragmented by traditional ToF-SIMS techniques. Another surface characterization technique is matrix assisted laser desorption ionization (MALDI). MALDI uses a laser beam to energize molecules in the surface of a sample, thereby ejecting particles to be detected by a ToF analyzer. Preparing samples for analysis in MALDI involves embedding the substance to be

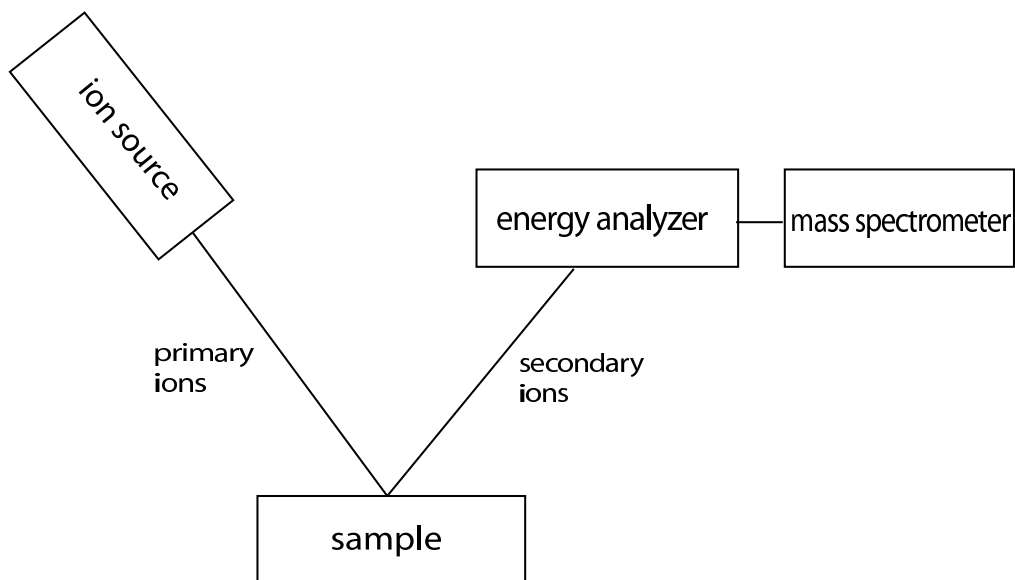


Figure 1: Simple schematic of SIMS apparatus.

studied, known as the analyte, in an appropriate crystal, known as a matrix, which aids in particle liftoff. A simple diagram of MALDI is shown in Figure 2. It has been shown to analyze unfragmented molecules that are beyond the upper mass limit for ToF-SIMS (in the 10,000 amu range). The large spot size of the laser in MALDI limits its imaging capabilities. An effort has been made to combine ToF-SIMS and MALDI to create a new analysis tool that has the mass range and gentle liftoff of MALDI and the precision of ToF-SIMS by preparing the sample using MALDI techniques, then examining these crystals through SIMS. This method is called matrix enhanced secondary ion mass spectrometry (ME-SIMS).

One popular UV MALDI matrix is 2,5 dihydroxybenzoic acid (2,5 DHB). UV MALDI uses high energy, short wavelength lasers which only penetrate 100 nm into a sample surface [4], much like the primary ions in SIMS. The behavior of 2,5 DHB in ToF-SIMS has not been examined, but is key to knowing the potential of ME-SIMS using this matrix in biological applications. Wu and Odom measured the efficiency of MESIMS by embedding peptides, proteins, and nucleic acids in common MALDI matrices, and found 2,5 DHB to be the most effective matrix [1]. They were successful in analyzing molecules up to 10,000 amu in mass. ME-SIMS is generally found to be inefficient, which could be due to molecule desorption or ionization. Garrison used molecular dynamics to analyze molecular liftoff processes in MALDI and SIMS. Her findings suggest that the basic differences in the physics of these two

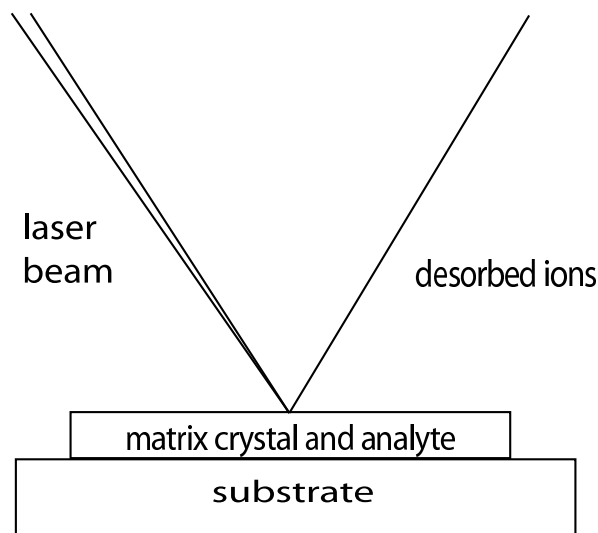


Figure 2: Simple schematic of MALDI.

surface analysis techniques contribute to the upper mass limit of SIMS. The SIMS primary ion initiates a cascade of individual collisions which ejects fragments of molecules from the surface of the sample. The laser beam in MALDI energizes molecules on the surface and deeper within the matrix at roughly the same time. These energetic particles then work collectively to eject whole analyte molecules from sample [3].

The crystalline structure of 2,5 DHB makes it convenient to study for surface damage. Crystals are easy to grow and have surface regularity on the nanometer scale. The surface topography of individual crystals was found using atomic force microscopy (AFM). These crystals were subsequently subjected to ion bombardment in the ToF-SIMS apparatus. The matrix surface was then studied again to note differences in surface roughness. The size and shape of the craters caused by incident ions predicts of the potential of ME-SIMS. These craters show the amount of material released from the surface per ion collision, which predicts the ability of large biomolecules to escape the crystal surface under ion bombardment.

The AFM is ideal for studying the surface structure of the 2,5 DHB crystals. Because the AFM does not cause surface charging, the insulating crystals do not need to have a metallic coating. Scanning electron microscopy (SEM) needs a conductive surface in order to create an image. To make SEM images of an insulating material such as 2,5 DHB, a layer of a metal such as gold must be sputtered on its surface. A metallic coating must be at least 10 nm thick to guarantee all surfaces are evenly coated. Thinner layers may be sputtered,

but the crystals often charge, making the image too bright and difficult to focus. A layer of acceptable thickness may fill the craters caused by the ion beam, thus making the study ineffective. All crystals imaged in the SEM were sputter coated with ~ 1 nm of Au. One drawback of the AFM is that it is difficult to identify spacial location of the image. This was overcome by etching a mark into the substrate prior to study.

Later sections describe the physics behind time of flight analysis and atomic force microscopy, and the ionization and liftoff processes in MALDI and SIMS. An outline of the method used to grow 2,5 DHB crystals, and their subsequent analysis is then presented. The effect of the SIMS environment on the crystal is discussed, along with the consequences of this effect in determining the volume of material ablated by each ion impact. Finally, suggestions for further experimentation on matrices when used in ToF-SIMS are made.

2 Underlying Physics

Molecular dynamics (MD) has been used to model molecular liftoff mechanisms for both SIMS and MALDI. MD integrates classical equations of motion over all particles in the system. In ToF-SIMS, an energetic ion collides with the sample surface, transferring its energy to the atoms and molecules in the surface and giving them enough energy to escape into the vacuum. Figure 3 is a molecular dynamics (MD) simulation of a sample surface at time $t = 0$ ps and at a later time $t = 1$ ps [6]. Some of the ejected particles are ionized, and then the ionized particles are accelerated through an electric field to a detector which uses basic physics to calculate the mass to charge ratio of the particle. The detector measures the time t each ion takes to travel a distance L to the detector, and can therefore calculate the mass m of the particle. The relationship between energy E each charge z is accelerated to and t is:

$$E = \frac{m\nu^2}{2} = \frac{mL^2}{2zt^2}, \tag{1}$$

where $\nu = \frac{L}{t}$. This mass to charge ratio makes it possible to characterize the surface composition of a sample with great accuracy [5]. In MALDI analysis a pulsed laser beam strikes a crystallized matrix embedded with analyte. The beam energizes molecules in the sample, causing the analyte to lift off unfragmented [6]. Figure 4 is an MD simulation of a sample surface after laser desorption. Both analysis techniques use time of flight analyzers. The

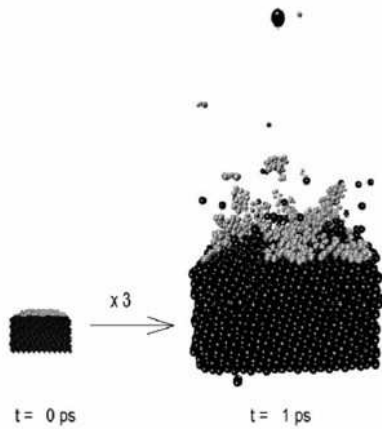


Figure 3: Molecular dynamics diagram illustrating SIMS molecular desorption process. The spheres represent molecules in a sample. Shown at time $t = 0$ ps and $t = 1$ ps [6].

physics of molecular liftoff and ionization is significantly different, so MALDI mechanisms will first be discussed, followed by SIMS mechanisms.

2.1 Ionization

Because both MALDI and SIMS use ToF analyzers, the ionization efficiency is an important factor for the overall efficiency of each analysis method. If the particles that are ejected are not ionized, they can not be detected by the ToF analyzer. In both MALDI and SIMS the ionization efficiency is low. The fraction of charged particles in SIMS is 10^{-6} - 10^{-1} [5].

In MALDI, the laser absorption by the sample surface causes a dense, energetic plume of matrix and analyte molecules to be ejected. This plume contains both ionized and neutral particles. The detection of ions increases faster than the amount of ablated material, therefore a large proportion of the analyte molecules detected are thought to be ionized through collisions with matrix ions in the plume [1]. The laser fluence threshold for ablation is lower than that for ion detection, which suggests that there are unabsorbed photons remaining after the plume is created. Molecules may also be ionized by absorbing these photons while in the plume [7].

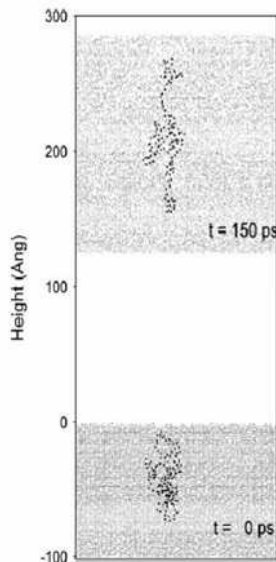


Figure 4: Molecular dynamics diagram illustrating MALDI molecular desorption process. The analyte molecule is shown embedded in the matrix at time $t = 0$ ps, and in the plume at $t = 150$ ps [6].

Wu and Odom [1] note that there is a distinct difference in ionization mechanisms between SIMS and MALDI. The primary ion beam does not cause the ejection of enough particles to facilitate plume interactions. Also, there are no photoionization processes in SIMS. They therefore hypothesize that the molecules detected by the ToF analyzer are not ionized during or after primary ion impact, but are already ionized while still embedded in the matrix. This explains why matrices with many donor protons such as 2,5 DHB create the highest ion yields in ME-SIMS. The maximum ionization efficiency of ME-SIMS is low, however, so this technique is not widely used.

2.2 Molecular Liftoff

In MALDI, laser pulses with approximately $5 \mu\text{J}$ energy bombard a crystallized matrix embedded with analyte. Photons of approximate energy 4 eV penetrate the surface of the matrix, transferring their energy to the molecules in the sample. Garrison *et al.* [6] used MD to examine molecular liftoff in MALDI and SIMS to attempt to determine why the upper mass limit differs so greatly between them. They modeled liftoff processes in MALDI by giving each molecule in the system translational degrees of freedom, and representing the

analyte molecule as a ball and spring. Their simulation showed desorption of molecules with masses of 30,000 amu. The high mass of these ejected molecules is due to the concerted effort of the photoenergized molecules in the matrix.

Energetic primary ions in SIMS cause a series of collisions that transfer the energy of the ion to molecules in the surface. These collisions allow for surface molecules to be ejected into the vacuum towards the detector. Garrison describes these collisions as a “pool game with sticky balls” [3]. These collisional cascades have been modeled using MD [3][5]. Delcorte modeled massive molecule desorption in SIMS and found the high mass limit to be 2,000 amu. This simulation found that higher energy primary ions caused material to be ejected from a larger area. Ions with energy of 5 keV caused ejection of particles from a radius of 25 Å area surrounding the impact point, whereas ions with energy of 500 eV limited ejection to 15 Å around the impact point [2]. Higher energy incident ions cause collision cascades which penetrate deeper into the sample, thus releasing more particles from the surface. The high energy of the ion impact and subsequent collisions can break apart molecules near the impact site. Therefore, particles ejected from the impact site are mostly atoms, whereas those released from the surrounding area are whole and fragmented molecules. This higher energy, however, fragments more molecules, and can heat the fragile biomolecules causing more damage to the analyte [5]. Garrison’s MD modeling shows that SIMS collision cascades occur on a sub-picosecond time scale which minimizes heat induced damage to molecules [3]. High mass ions are difficult to obtain by ToF-SIMS alone. The measurements made in this experiment will characterize the behavior of a matrix crystal in SIMS. The existence of craters caused by primary ions deeper than 10 nm would indicate that SIMS is not strictly a surface tool when used in conjunction with matrices, which would lead to the belief that the high mass inefficiency in ME-SIMS is not due to molecule desorption.

2.3 Volume of Ablated Material

Fournier *et al.* [7] studied the behavior of 2,5 DHB in MALDI and found that the volume of material irradiated from an area S_i in the sample is dependent on the fluence Φ_i of the laser and the threshold fluence for ablation Φ_{th} . The relation they used is:

$$e_i = A_0(\Phi_i - \Phi_{th})^n, \tag{2}$$

where e_i is the depth of the crater ablated by each pulse, and A_0 and n are adjustable parameters. The value of n varies from $n=1$ to $n=4.5$ depending on the angle of incidence of the laser on the surface, and thus the absorbed energy density. High n corresponds to the laser being near perpendicular to the surface. The parameters were adjusted after each simulated laser shot to account for changes in angle of incidence. Fournier *et al.* found that for laser shots of energy $4.7 \mu\text{J}$ and spot size of approximately $100 \mu\text{m}$ diameter, the average ablated volume per shot was $387 \mu\text{m}^3$ [7], or $80 \mu\text{m}^3/\mu\text{J}$.

The volume of material ablated in SIMS will indicate whether large molecules can escape the surface of the matrix. In SIMS, primary ions have energy of 22 keV, or $3.52 \times 10^{-9} \mu\text{J}$. If we use the MALDI value for volume ablated per μJ (approximately $100 \mu\text{m}^3$), then each incident ion would presumably ablate $3.52 \times 10^{-7} \mu\text{m}^3$. Assuming molecules desorb from within 5nm of the impact site in SIMS [8] we can expect craters of depth 6-10 nm per incident ion. Because the presence of a matrix causes particles to be ejected from deep within the sample, the surface sensitivity of SIMS is degraded. This penetration depth, however, should allow large molecules to be ejected from the sample.

2.4 Atomic Force Microscopy

Atomic Force Microscopy (AFM) is a reliable and precise method of surface analysis. Much like a record player, the AFM scans the surface of the sample with a nanometer-scale tip on a cantilever, and a laser beam is used to measure the vertical deflection of the cantilever at each point. Figure 5 shows a schematic of an AFM. The AFM is capable of measuring many aspects of a sample from elasticity to friction to nanoscale topography and roughness. It is the latter of these that this project utilizes. The most common way to measure the topography of a surface is to use “tapping mode.” This mode has the cantilever oscillating at resonance (around 250 kHz) and recording the height of the surface when the tip touches on each downward stroke of the tip. This form of AFM has minimum distortion from drag, as well as reduced wear on the tip. Under average conditions, the AFM can scan areas from $15 \mu\text{m} \times 15 \mu\text{m}$ to $100 \text{ nm} \times 100 \text{ nm}$.

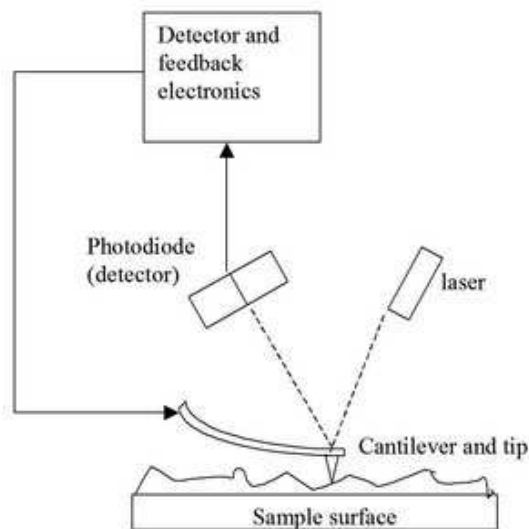
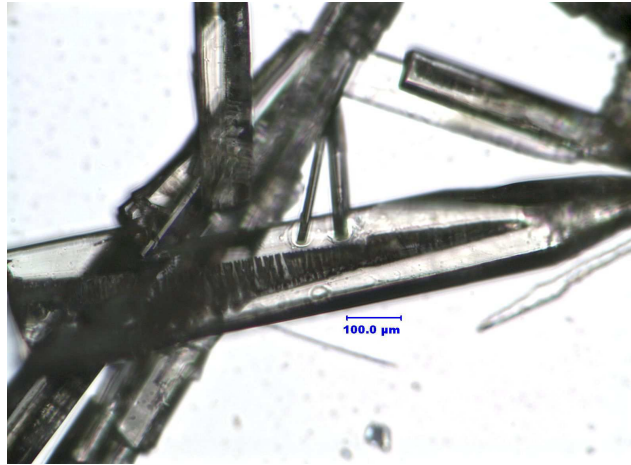


Figure 5: Schematic of an AFM apparatus [9].

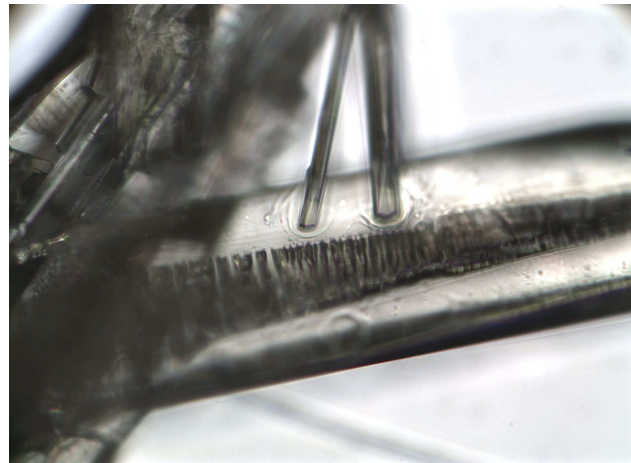
3 Crystal Growth and Surface Analysis

The 2,5 DHB purchased from Acros Organics (Morris Plains, NJ) was used without further purification. Crystal growth procedures were directly adopted from previous ME-SIMS research [1]. A 6 μL sample of .5M solution of 2,5 DHB with 50% water and 50% acetonitrile was placed on a glass slide and allowed to crystallize at room temperature. Within fifteen minutes, macroscopic crystals (5 mm x 1 mm x 1 mm) formed. These crystals were studied under an optical microscope. This same method was used to grow crystals on substrates for analysis. Clean 1 cm x 1 cm silver foils and silicon wafers were chosen as sample substrates because of their common use in ToF-SIMS analysis. An air duster detached loose crystals from the sample, leaving only those crystals sturdily attached to the substrate.

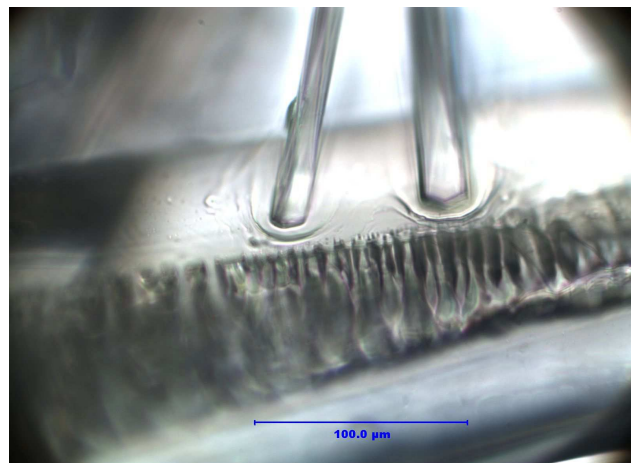
The crystallized samples were then taken to the Applied Research Center (ARC) in Newport News, VA for further analysis. Crystals on both the Si and Ag substrates were examined with the Axiolab Transmitted and Reflected Light Microscope (Zeiss) apparatus. Images of several crystals were made with 100x, 200x, and 400x magnification to study the roughness and structure of the individual crystals, as well as their location and orientation on the substrate for later identification. Figure 6 shows optical microscope images of a set of newly grown crystals at various magnifications. These images demonstrate how “road maps”



(a) magnification: 100x. bar = 100 μm



(b) magnification: 200x



(c) magnification: 400x. bar = 100 μm

Figure 6: Optical microscope images of 2,5 DHB crystals on Si substrate.

of the crystals were developed. Distinguishing shapes, sizes, and orientation of crystals were used to identify crystals in the poorer magnification of the AFM and ToF-SIMS. Note the two smaller crystals attached to the side of the larger crystal in Figure 6.

The samples were then studied in the atomic force microscope (AFM). A variety of surface structures were found. Extremely flat surfaces were easily found, and spread over several hundred nanometers. Figure 7 shows AFM images of the surface of a 2,5 DHB crystal on an

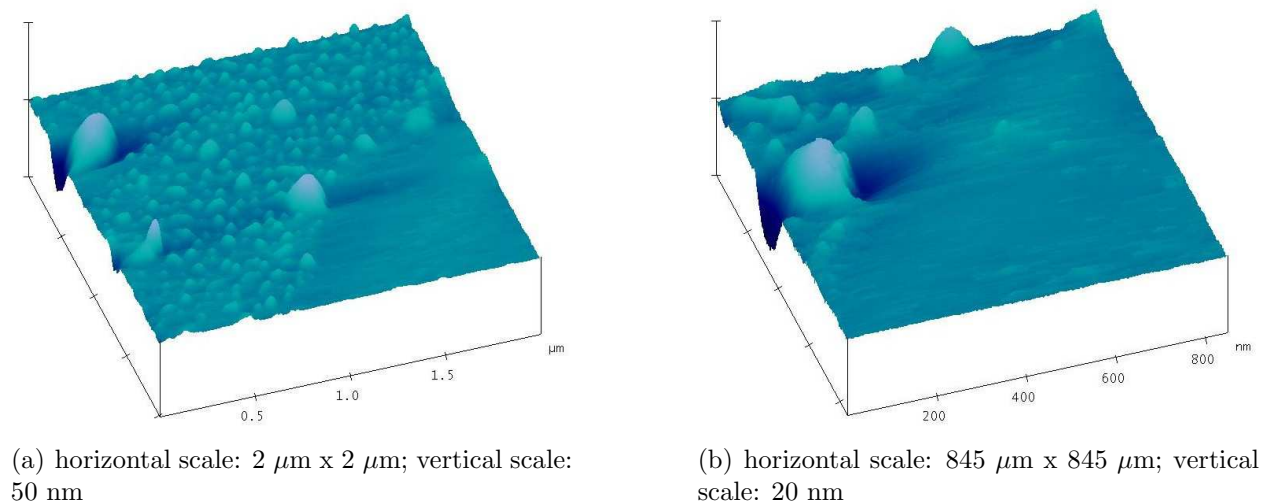


Figure 7: AFM images of a smooth area on the surface of a 2,5 DHB crystal on Ag substrate.

Ag substrate. The surface has an area with regularly spaced small peaks (~ 10 nm) adjacent to an area with no surface variation on the nanometer scale. The next step was to develop a methodology to find a patch of the crystal surface that was both flat and re-identifiable. This is key because it allows for a before and after view of the same area, guaranteeing that differences in surface topology are due to the ion beam in ToF-SIMS, not just variations in topology from one spot on the crystal to another.

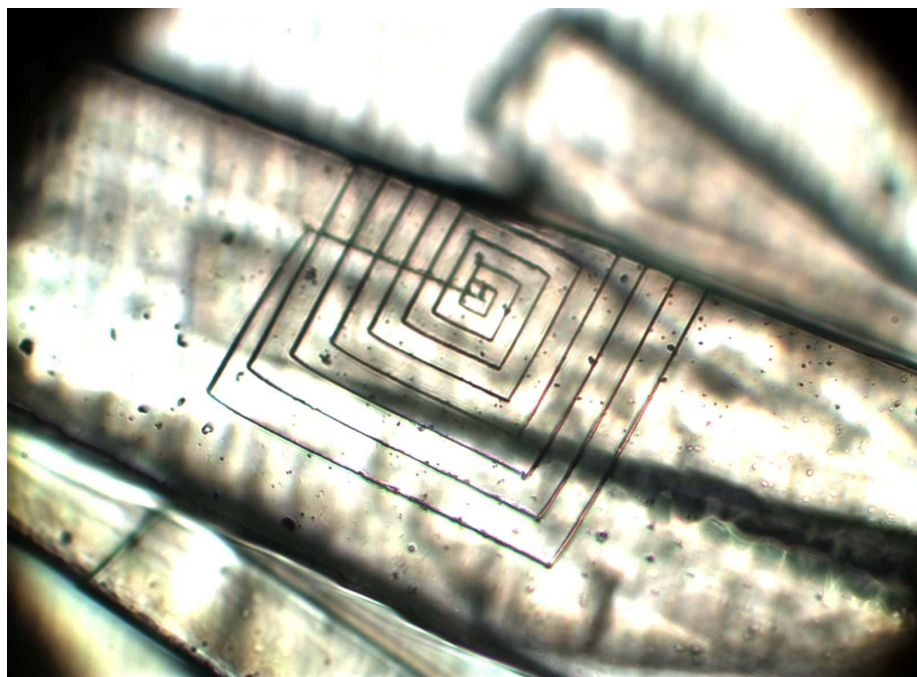
Because the AFM works on the nanometer to micron scale, it was necessary to mark the crystals on a comparable scale. This can be done by putting the tip in direct contact with (or pressing into) the sample, and then moving it along the surface, etching a pattern. When beginning an AFM scan, it is necessary to show the instrument where the surface is (the “focus surface” function) and where the tip is (the “locate tip” function). When locating the tip, the cantilever moves in a square spiral motion, allowing for one to find the tip if it is off screen. If when focusing the surface one focuses on a point below the surface,

the tip touches down on the crystal. One can then “locate tip,” etching this square spiral into the surface. Figure 8 shows one of these etchings as seen with the optical microscope. The distance between lines in this pattern is $\sim 10 \mu\text{m}$. Once these etchings in the surface are made, it is possible to scan a large area ($\sim 15 \mu\text{m} \times 15 \mu\text{m}$) within this pattern, and then zoom in to smaller areas until sufficient resolution is obtained. This process is shown in Figure 9. Figures 9 (b) and (d) are zoomed in areas of images (a) and (c), respectively. Images (c) and (d) are were taken after removing the sample and reorienting it on the sample holder. All images are of the same area, identifiable by landmarks such as peak size, shape, and location, and the “hook” formation towards the center of the zoomed in images. The doubling of the peaks in image (d) is due to wear on the AFM tip.

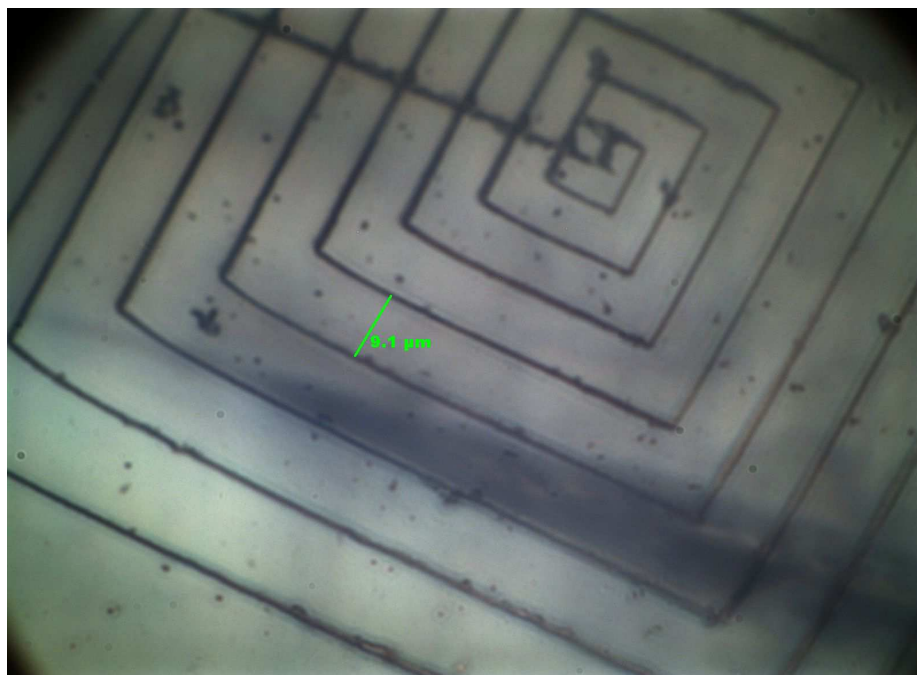
After locating and scanning a smooth surface on the AFM, the crystals were placed into the PHI THRIFT II Time of Flight SIMS (ToF-SIMS) apparatus. The chosen crystals were located through their general orientation and shape (as found on the Zeiss optical microscope) and sputtered for a range of times over a large area. The large area ensures that the chosen areas are covered, because location of a surface in the ToF-SIMS is difficult. The camera used to view the surface of the sample is poorly focused and the grating that holds the sample in place obscures the picture further. The Au source ion beam was run at 22 keV over a $200 \mu\text{m} \times 200 \mu\text{m}$ area for 5, 10, and 15 minutes. The vacuum in the ToF-SIMS is on the order of 10^{-10} Torr. The spectra and total ion images were obtained, but neither were used for this study.

The next step is to reanalyze the surface topography of the crystals in the AFM. Using the steps mentioned above, the same areas scanned before sputtering in the ToF-SIMS should be looked at again. The existence of new craters on the order of 100 \AA would suggest that large biomolecules may be desorbed from the matrix, thus showing that the inefficiency of ME-SIMS does not lie in molecular liftoff.

Scanning electron microscope (SEM) images of the crystals allow for a greater magnification range to be obtained. Some SEM images were made, but their quality is limited by charging of the crystal.

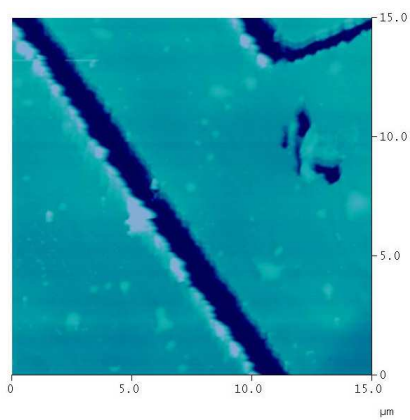


(a) magnification: 400x

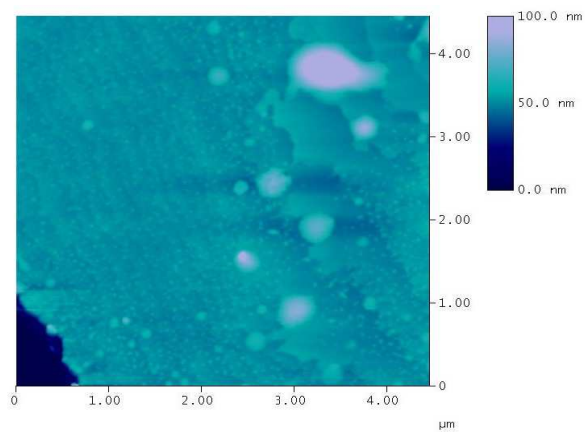


(b) magnification: 1000x. green line is 9.1 μm

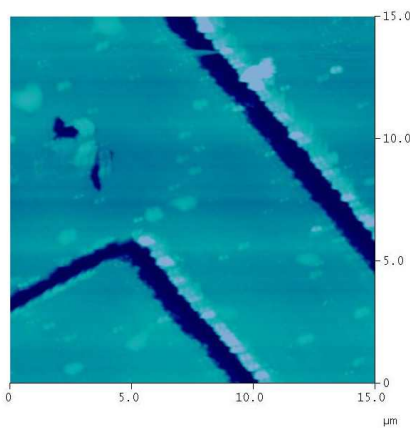
Figure 8: Light microscope image of etched 2,5 DHB crystal on Ag substrate.



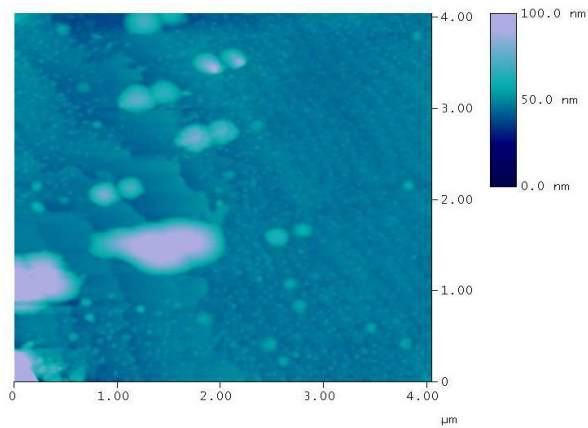
(a) 15 μm x 15 μm



(b) 4.5 μm x 4.5 μm



(c) 15 μm x 15 μm



(d) 4 μm x 4 μm

Figure 9: AFM images of 2,5 DHB crystals on Ag substrate.

4 Results

The 2,5 DHB crystals grown on the Si and Ag matrix were found to range in size from $15\ \mu\text{m} \times 70\ \mu\text{m}$ to $0.5\ \text{mm} \times 3\ \text{mm}$. Crystals grew along the edges of each substrate, often overlapping. The smoothest crystals tended to be the smaller crystals that commonly grew at the base of several larger ones. Large crystals show signs of fracturing and fissuring within the crystal due to stress during growth, but have mostly smooth surfaces. The smallest crystals are optically smooth throughout, having apparently planar surfaces. Figure 10 shows the

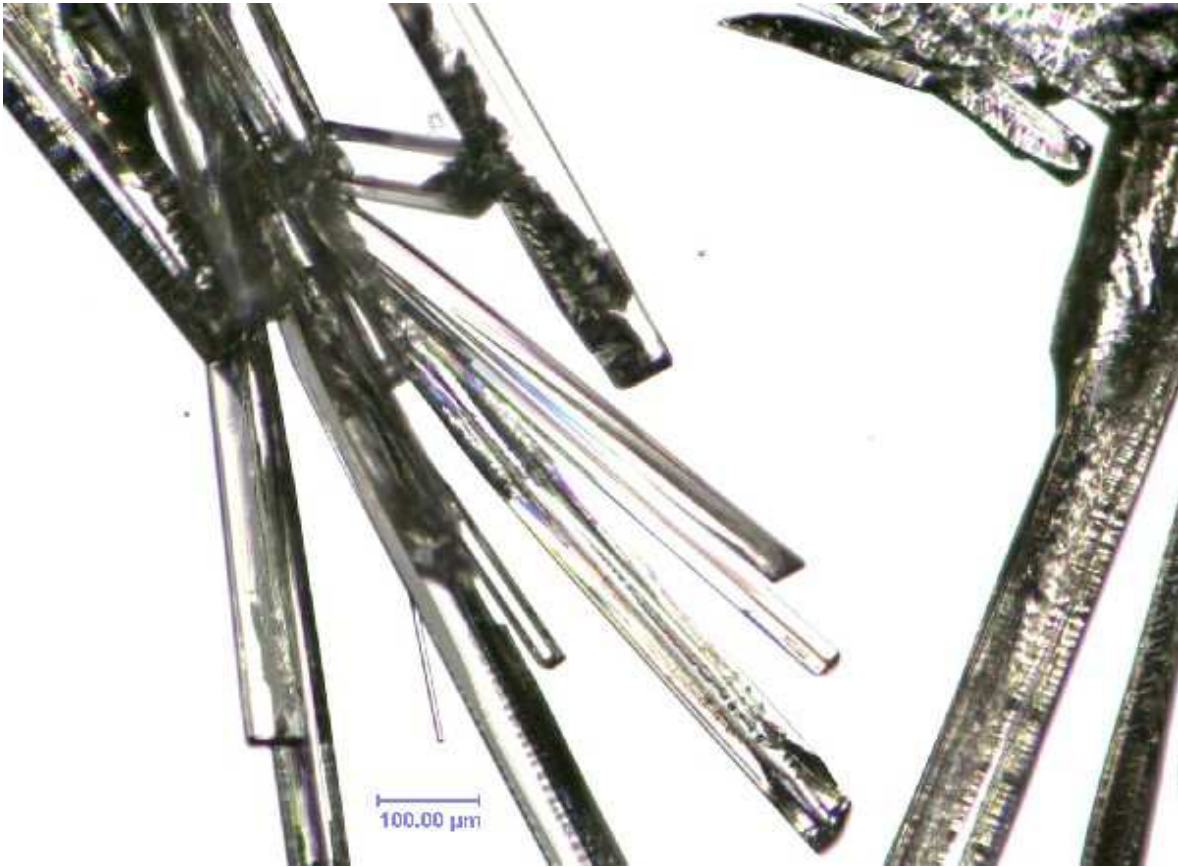
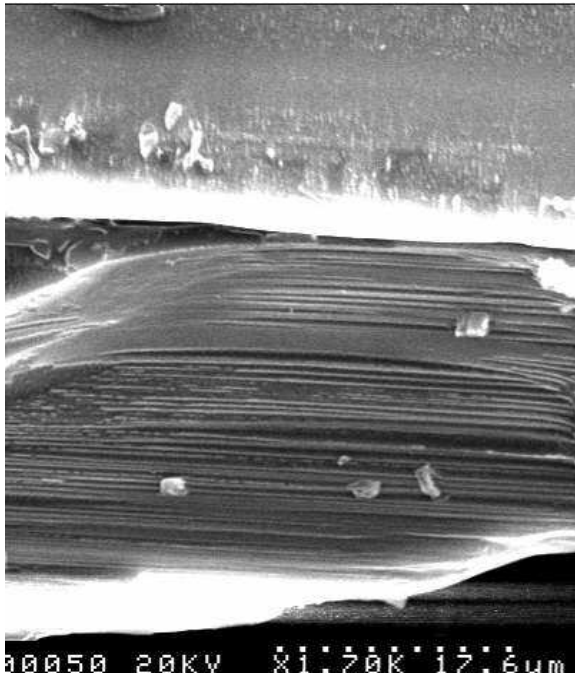


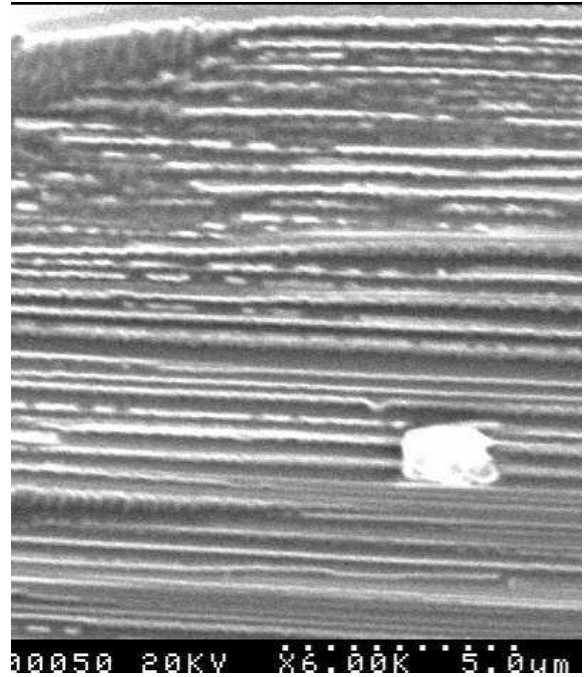
Figure 10: Light microscope image of 2,5 DHB crystals on Ag substrate. Magnification 100x.

typical growth pattern of the matrix crystals. Note the clarity of the smallest crystals and the stress marks on the larger ones.

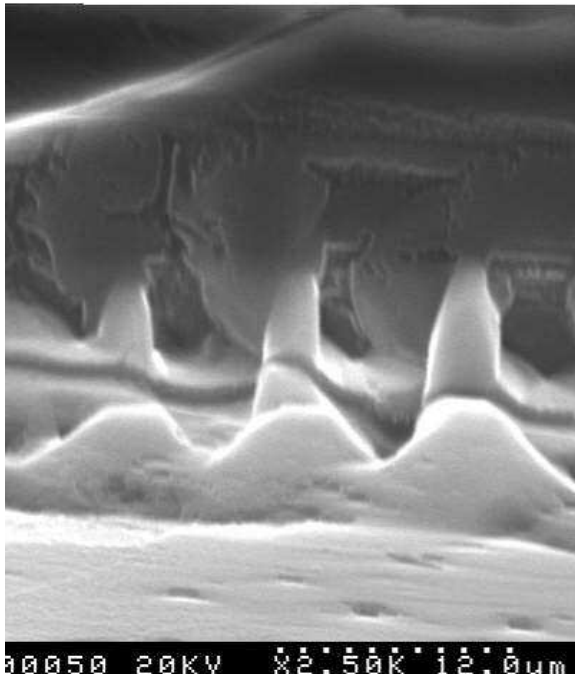
SEM images can be used to show the growth pattern of rougher surfaces on larger areas than the AFM. Figures 11 (a) and (b) show natural striations in the surface of a crystal.



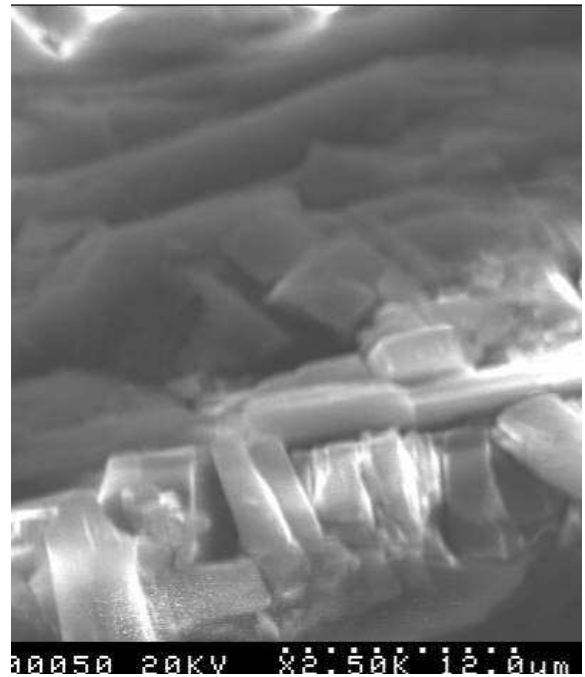
(a) dashed line = 17.6 μm



(b) dashed line = 5 μm



(c) dashed line = 12 μm



(d) dashed line = 12 μm

Figure 11: SEM images of Au coated 2,5 DHB crystals on Si substrate.

Figure 11 (c) shows an imperfection of the crystal due to the stress inherent in crystal growth. Figure 11 (d) shows the fractured edge of a broken crystal, demonstrating 2,5 DHB's tendency to splinter when broken.

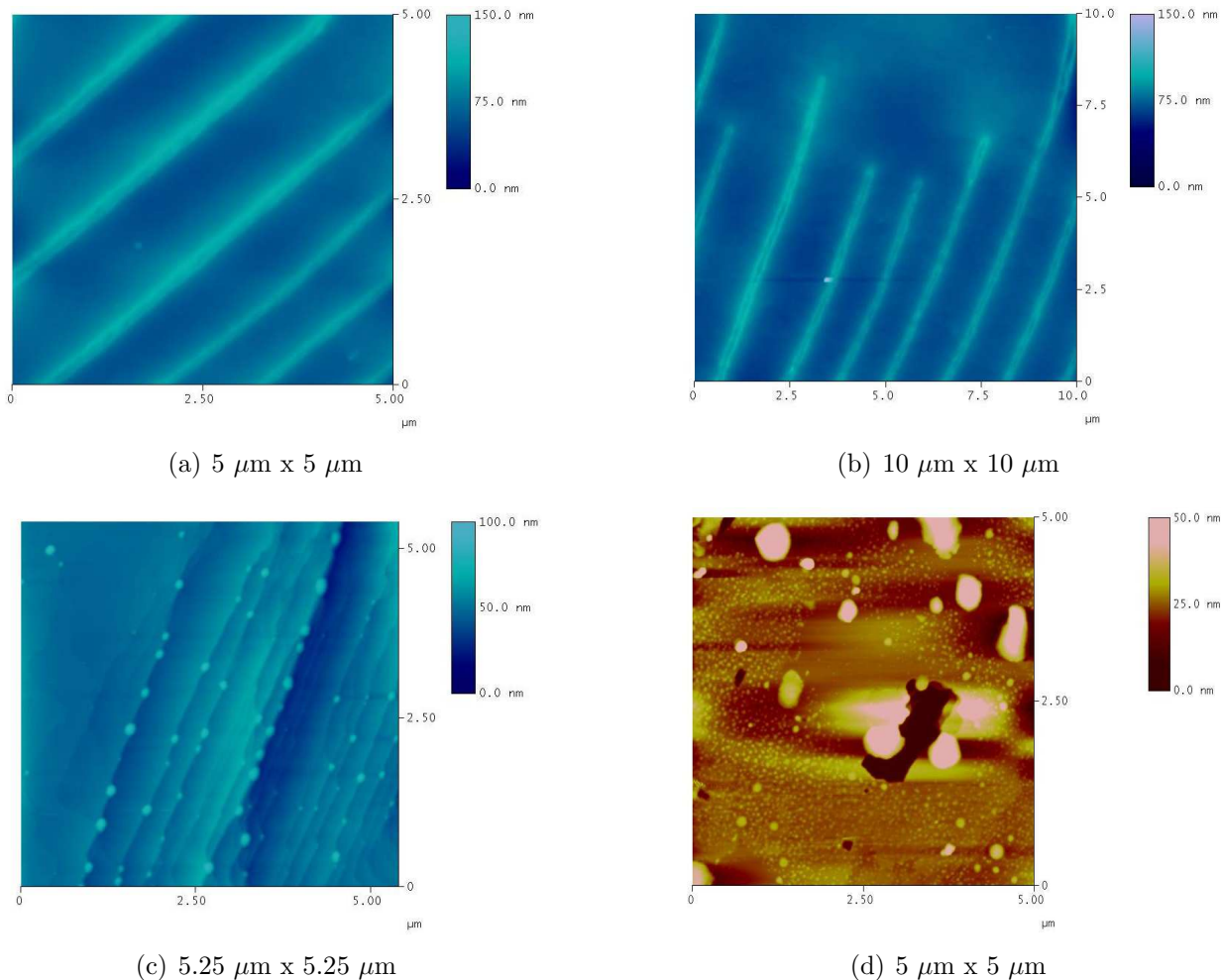


Figure 12: AFM images of 2,5 DHB crystals on Si and Ag substrates.

AFM analysis of the crystals showed a variety of surface topographies. The substrate seemed to have some effect on surface topography, but the surfaces varied greatly from crystal to crystal, as well as on single crystals. Figure 12 illustrates the variety of these surface patterns. Figure 12 (a) and (b) show crystal surface which have grown with straight, regularly spaced ridges about 50 nm high every $1\ \mu\text{m}$. Figure 12 (c) shows a crystal surface with crystallographic planes that have grown at an angle to the surface, with peaks dotting the edge of each plane. Figure 12 (d) shows a surface that is flat with regularly spaced small

(~ 10 nm) peaks and a variety of large (~ 30 nm) deformations. On the nanometer scale, perfectly planar surfaces are fairly common on the crystals grown on the Ag substrate, while the surface of crystals grown on Si had a rougher surface structure. Figure 13 shows 10

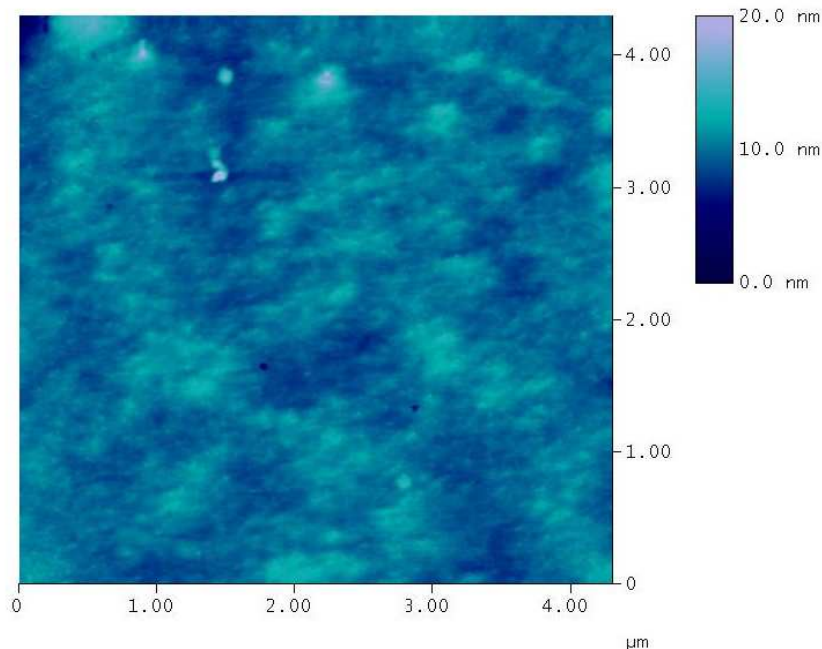
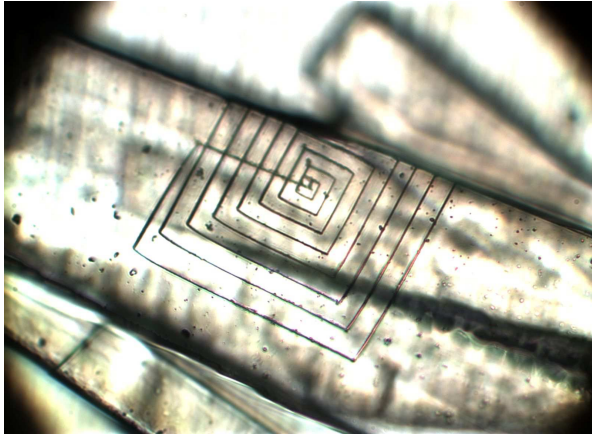


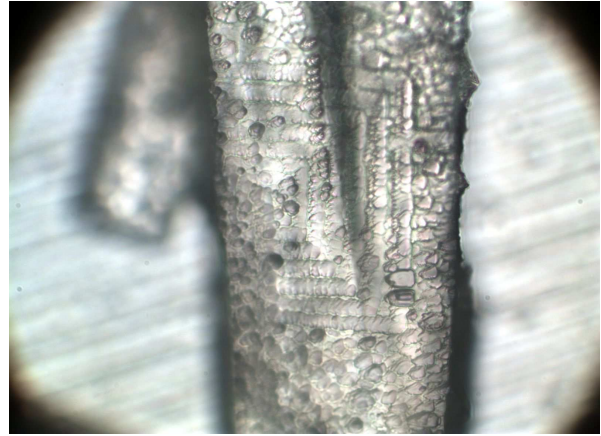
Figure 13: AFM image of 2,5 DHB on Si substrate. $4.5 \mu\text{m} \times 4.5 \mu\text{m}$.

nm variations over ~ 100 nm on the surface of 2,5 DHB on Si. Both the planar and rough topographies should be acceptable for the purpose of this study because of the regularity and scale of the structures.

When the crystals were placed in the ToF-SIMS, their surface structure changed dramatically. Figure 14 shows images taken on a light microscope of the corrosion of the surface of a single crystal. The differences in surface appearance before and after insertion in the SIMS instrument are striking. The craters are found on every crystal on each sample placed in the ToF-SIMS, regardless of whether that area was bombarded by the ion beam or not. These extreme changes to the topology of the crystal make it impossible to analyze the effects of the ion beam on the crystal. This surface destruction appears to be damage due to the high voltage bias on all samples in SIMS. This phenomena and steps to overcome it will be further explored in the discussion section.



(a) etched crystal before SIMS. magnification: 400x



(b) etched crystal after SIMS. magnification: 400x

Figure 14: Optical microscope images of an etched 2,5 DHB crystal on Ag substrate, pre and post insertion in the SIMS instrument

5 Discussion

Some mechanism within the ToF-SIMS apparatus (but separate from the incident ion beam itself) causes complete destruction of the surface of the 2,5 DHB crystals. The severity of the deterioration is time dependent. Figure 14 (b) shows a crystal after several days in the SIMS instrument, Figure 16 (c) shows a crystal after 24 hours in the SIMS, and Figure 17 shows a crystal after only a few hours. From these images it is clear that the amount of surface corrosion decreases with time in the SIMS. The surface deterioration makes the methodology developed to see the effects of the ion beam on the crystals impossible. Figure 14 is an image taken with an optical microscope, showing the surface utterly changed from its previous state; even the deepest etchings made by the AFM are muddled and difficult to recognize. Figure 15 is an AFM scan of a 2,5 DHB crystal on an Ag substrate after analysis in SIMS, illustrating that AFM scans of the surfaces of the crystals show that they no longer retain any crystallographic structure on the nanometer or micron scale and can be too rough to be analyzed. Because of this, it is impossible to find the area scanned prior to ToF-SIMS, and to determine what surface destruction is due to the ion beam and what is due to some other factor.

There are a myriad of possible reasons for this sort of deterioration. They include the high vacuum of the ToF-SIMS chamber, the background voltage on the sample holder that

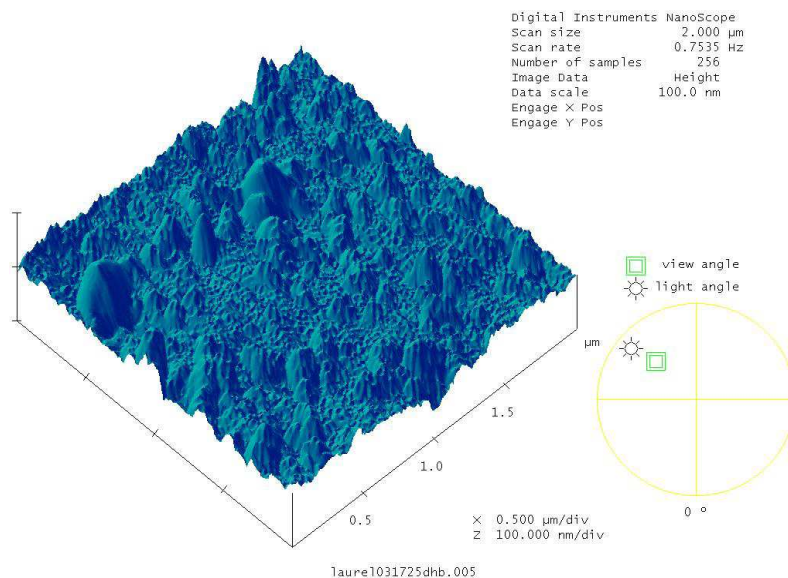
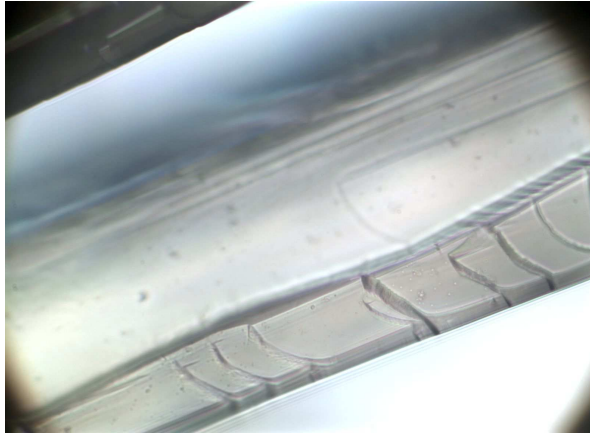


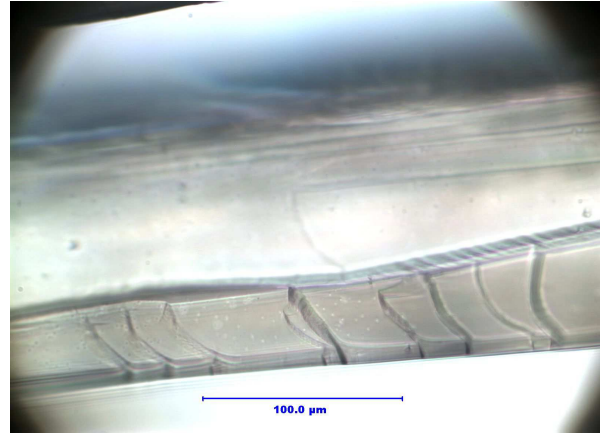
Figure 15: AFM image of 2,5 DHB on Ag substrate after several days in the SIMS instrument. horizontal scale: 2 μm ; vertical scale: 100 nm.

accelerates the ion beam to the surface, implications of these two factors, or some unknown aspect of the ToF-SIMS environment

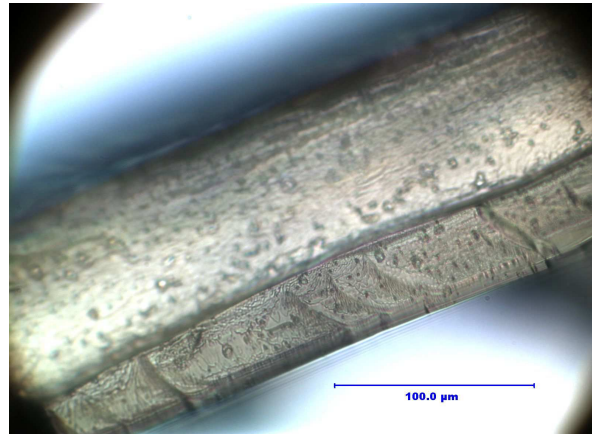
The vacuum in the ToF-SIMS chamber is on the order of 10^{-10} Torr. This high vacuum may cause sublimation of the crystal itself, or small pockets of solvent within the crystals may vaporize and burst through the surface. Because other studies of the effects of MALDI (which also operates under a high vacuum) on 2,5 DHB have been performed and none mention this kind of surface damage [7], the vacuum seems an unlikely source of destruction. Figure 16 shows light microscope images of a crystal before vacuum, after low vacuum, and after high vacuum. Figure 16 (a) shows the fresh crystal. The sample was then placed in a vacuum chamber (on the order of 10^{-4} Torr) for an hour. Figure 16 (b) is the same crystal after removal from this vacuum, and shows no surface deterioration. The same crystals were then put into the ToF-SIMS vacuum chamber overnight. Figure 16 (c) shows the crystal after twenty four hours in this high vacuum, which exhibits the same sort of surface corrosion seen previously. Figure 17 is a collection of images of these crystals taken with the SEM. Figure 17 (b) is an expanded image of the left side of the crystal in (a), and (c) is an expanded image of the right side of the crystal in (a). The variety of surface damage caused by the SIMS ranges from removal of 3 μm long strips of the top crystallographic plane to distinct 1 μm diameter craters formed in the surface. Because the lower vacuum showed no



(a) new crystal. magnification: 400x.

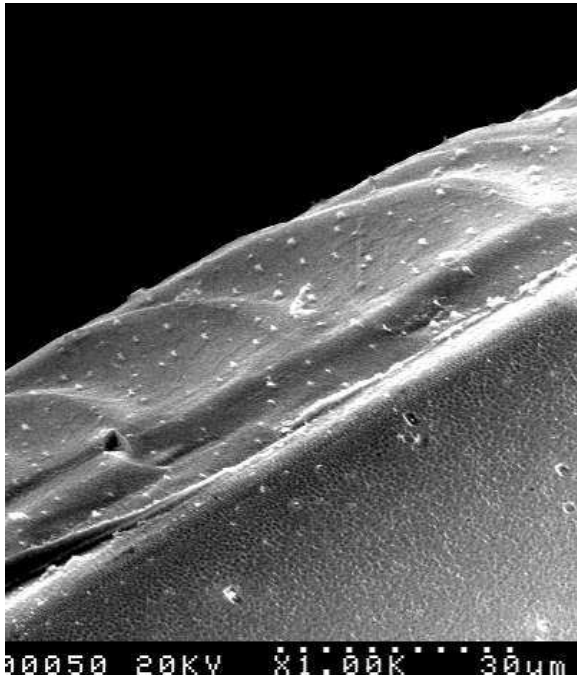


(b) crystal after 1 hour in low vacuum. magnification: 400x. bar = 100 μm

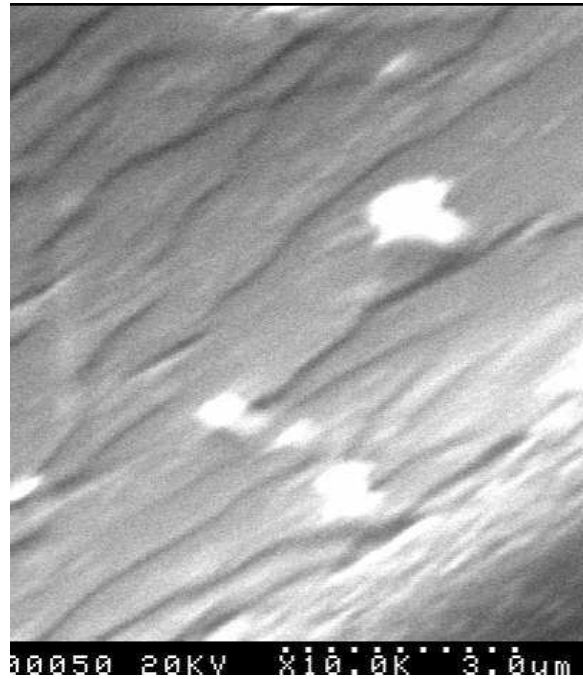


(c) crystal after 24 hours in SIMS. magnification: 400x. bar = 100 μm

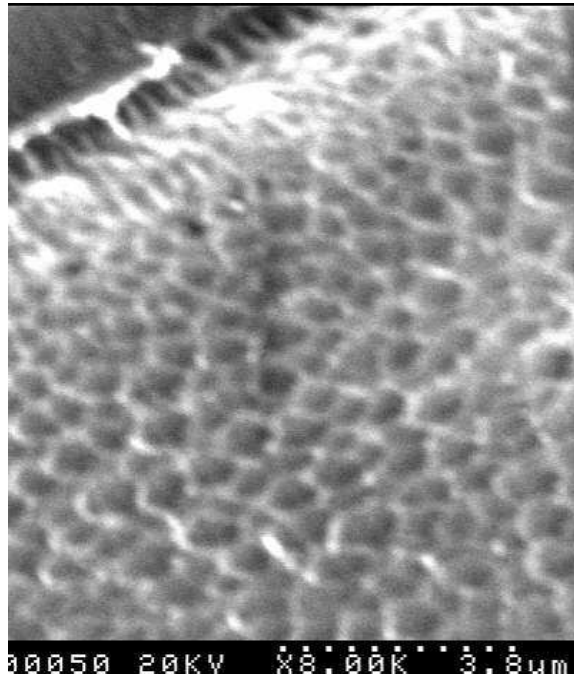
Figure 16: Optical microscope images of 2,5 DHB on Si substrate



(a) dashed line = 30 μm



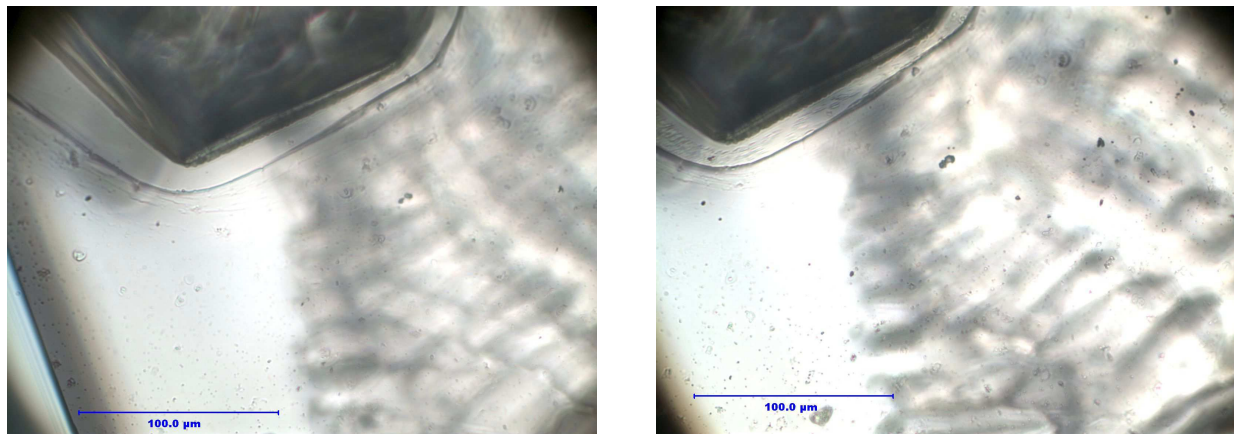
(b) dashed line = 5 μm



(c) dashed line = 3.8 μm

Figure 17: SEM images of Au plated 2,5 DHB on Si after 24 hours in the SIMS environment.

signs of destruction of the crystals, it seems unlikely that the ToF-SIMS vacuum itself would cause the surface deterioration. In case time is a factor, a new set of crystals were grown, imaged under an optical microscope, and then placed in the vacuum chamber for 24 hours. The crystals were then removed from the vacuum chamber and studied for surface changes with the optical microscope. Figure 18 shows these crystals, demonstrating that the vacuum caused a few new craters on the surface of the crystals, but the damage was far less extensive than that created by the ToF-SIMS.

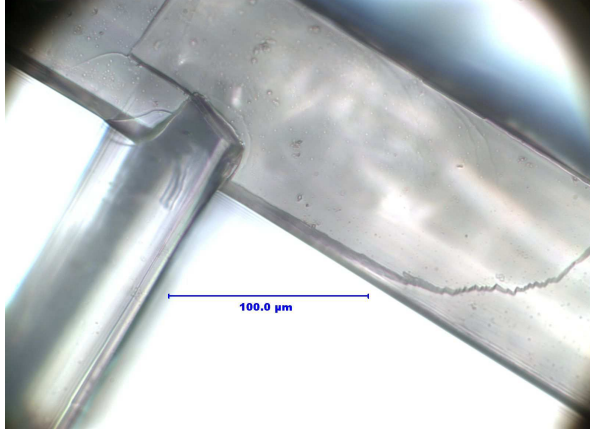


(a) pre-low vacuum. magnification 400x. bar = 100 μm

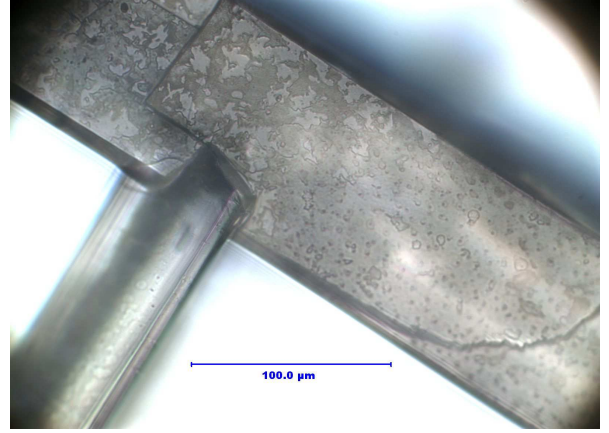
(b) post-low vacuum. magnification 400x. bar = 100 μm

Figure 18: Optical microscope images of 2,5 DHB on Si substrate before and after 24 hours in 10^{-4} Torr.

Each time the 2,5 DHB samples were placed in the ToF-SIMS, other samples were being analyzed using the SIMS. During SIMS analysis, a high voltage is placed behind the sample. The design of this instrument makes this high voltage run behind all samples in the sample holder for the duration of all runs. This could cause damage to the crystal surface because pieces of the matrix may charge and then be repelled from the high voltage behind the samples. Small chunks could thus break off of the crystal. Figure 19 (b) shows a crystal that was inserted in the SIMS instrument for 3 hours, with the high voltage on for 30 minutes. The surface of the 2,5 DHB looks like a jigsaw puzzle missing a few pieces. This is suggestive of charging damage because the shapes of the craters are not uniform, indicating that charging happened to random areas on the surface. Also, it appears as though each piece was removed from the same crystallographic plane, which shows that the surface broke where surface bonds are weakest.



(a) pre-high voltage. magnification 400x. bar = 100 μm



(b) post-high voltage. magnification 400x. bar = 100 μm

Figure 19: Optical microscope images of 2,5 DHB on Si substrate before and after 30 minutes on high voltage.

To see whether the voltage bias is a viable explanation for the surface damage of the crystals, a few rough calculations can be made. The electric fields E that build up on the surface of the crystal due to electrons attracted to it by the acceleration voltage V_{acc} must cause potentials less than the acceleration voltage. Thus

$$\int E \cdot dr = \Delta V = ER < V_{acc}, \quad (3)$$

where R is the radius of a crater caused by the voltage. The energy W stored in these fields is

$$W = \int \frac{\epsilon_o}{2} E^2 dt \approx \frac{\epsilon_o E^2}{2} \frac{2\pi R^3}{3}. \quad (4)$$

Combining (3) and (4), we find

$$W = \frac{\epsilon_o}{2} E^2 R^2 \frac{2\pi R}{3} < \frac{\epsilon_o}{2} V_{acc}^2 \frac{2\pi R}{3}. \quad (5)$$

The energy required to cause crater of radius R and depth of one monolayer can be approximated with

$$l\Delta V = l\Delta x\pi R^2 < W, \quad (6)$$

where ΔV is the volume of desorbed material, l is the latent energy and ΔX is the lattice separation of 2,5 DHB. Combining (5) and (6), we obtain a maximum radius of

$$R < \frac{\epsilon_o V_{acc}^2}{2l\Delta x}. \quad (7)$$

The maximum radius of the craters caused (and thus, the extent of damage) is proportional to the square of the applied voltage. The latent energy here is $0.125 \mu\text{J}/\mu\text{m}^3$ as calculated from Fourniers findings [7], the lattice spacing is $\sim 6.34 \text{ \AA}$, and the acceleration voltage is 10 kV. We thus find the maximum radius of craters to be $15 \mu\text{m}$. This is the same order of magnitude as the craters seen in Figure 19 (b).

To further check the validity of the charging damage hypothesis, we can find the approximate number of extra electrons each molecule has to gain to create these electric fields. We use

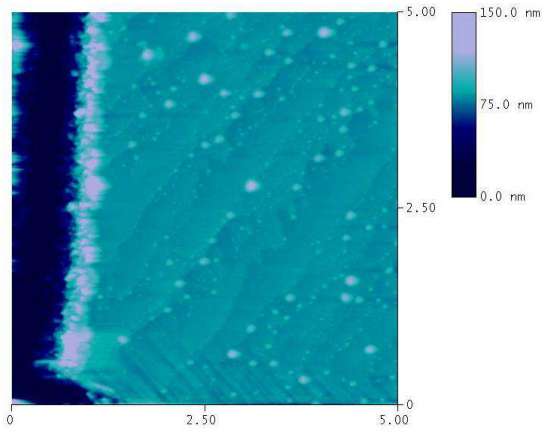
$$V = ER = \frac{\sigma R}{\epsilon_o} = \frac{Ne}{\pi(\Delta x)^2} \frac{R}{\epsilon_o} < V_{acc}, \quad (8)$$

where σ is the surface charge of the crystal, N is the number of electrons per molecule, and e is the charge of the electron. Solving for N we obtain

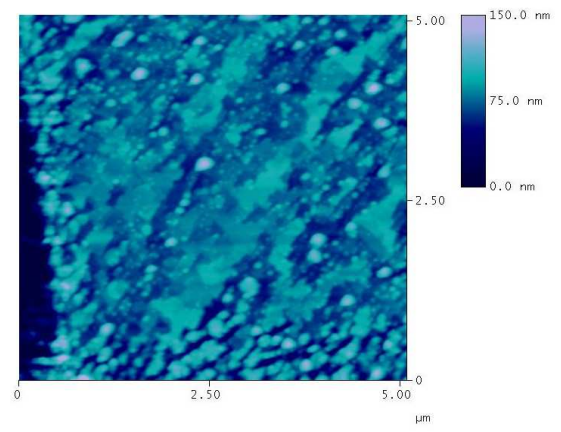
$$N < \frac{\pi\epsilon_o(\Delta x)^2 V_{acc}}{eR}. \quad (9)$$

This approximation tells us that each matrix molecule must have $\sim 4.6 \times 10^{-2}$ extra electrons to counter the applied acceleration potential. These calculations suggest that the applied voltage could indeed cause deterioration of the surface on the scale that is observed, though further tests are necessary to prove the correlation.

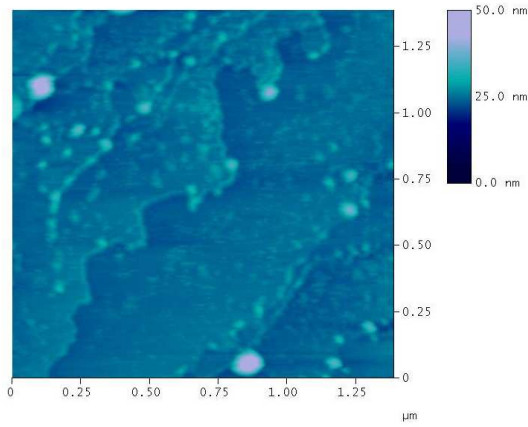
A set of new crystals was run in the ToF-SIMS instrument for the shortest cycle time possible, hoping that the high voltage damage would be minimized. The high voltage bias was on for ~ 15 minutes with the ion beam bombarding the sample for ~ 2 minutes. AFM images were taken of an area on the surface both pre-SIMS and post-SIMS. Figure 20 (a) shows the crystal surface prior to SIMS exposure. The gulley on the left side and bottom of the image is the etching made to mark the crystal. Figure 20 (b) is the same area after SIMS exposure. Surface characteristics such as the gulley and prominent peaks remained intact enough to recognize the area, but the general structure of the surface was dramatically changed. Figures 20 (c) and (d) are zoomed in images of approximately the same area; smaller identifying peaks were distorted beyond recognition by the SIMS. The surface damage is similar to that seen in the SEM image of a post-SIMS crystal, with strips of the top most crystallographic plane missing from the surface. This shows that even with shortest possible run time, there is too much deterioration due to high voltage to identify craters created by the impact of SIMS primary ions.



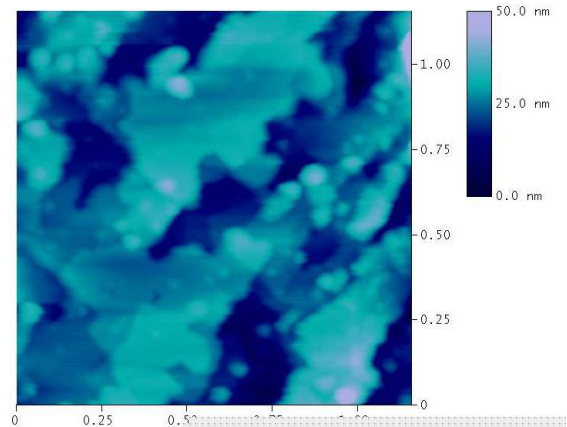
(a) pre-high voltage. $5 \mu\text{m} \times 5 \mu\text{m}$.



(b) post-high voltage. $5 \mu\text{m} \times 5 \mu\text{m}$.



(c) pre-high voltage. $1.5 \mu\text{m} \times 1.5 \mu\text{m}$.



(d) post-high voltage. $1.25 \mu\text{m} \times 1.25 \mu\text{m}$.

Figure 20: AFM images of 2,5 DHB on Si substrate before and after 20 minutes on high voltage

6 Conclusions

Many characteristics of ToF-SIMS make it ideal for analyzing the molecular surfaces of biomaterials. To optimize SIMS capabilities, it is necessary to develop techniques which allow large molecules to be ejected unfragmented. One possible option is to embed the analyte in matrix crystals, similar to those used in MALDI. Such a technique is called matrix enhance secondary ion mass spectrometry (ME-SIMS). The introduction of the matrix could serve many purposes, such as minimizing fragmentation of large, fragile molecules, and maximizing ionization of ejected particles. ME-SIMS has been found to be inefficient, and it is necessary to find out where this inefficiency lies before determining the potential of ME-SIMS for biological applications. The inefficiency may lie in the ejection of the molecules, or in their ionization. By studying the volume of ablated material from ion shots, it may be possible to determine whether large biomolecules may escape the matrix when bombarded with incident ions. One common MALDI matrix, 2,5 DHB, has shown potential in ME-SIMS [1]. There is an abundance of information on the behavior of 2,5 DHB when bombarded with laser pulses, including volume of ablated material per shot and shape of subsequent craters. There is little or no information on the behavior of 2,5 DHB when subjected to energetic ion bombardment, which would prove useful in analyzing the potential of ME-SIMS to extend the mass range of ToF-SIMS.

The methodology developed here makes it possible to find a specific area on a matrix crystal multiple times in the AFM. This is necessary in determining the nanometer scale change a surface undergoes in the ToF-SIMS. Because the surface of 2,5 DHB crystals changes dramatically on the micron scale due to some factor in the ToF-SIMS, the precision of AFM analysis isn't applicable until a method of eliminating damage to the surface is determined. It is first necessary to conclusively determine whether the acceleration voltage causes the surface deterioration. One way to test this is to apply a variety of electric potentials to 2,5 DHB crystals. The radius of craters caused should vary as the square of these potentials. If this relationship is shown experimentally, it may be inferred that the applied voltage causes the surface damage.

If it is indeed the acceleration voltage that causes the surface deterioration, then steps should be taken to eliminate this damage so that one can study the effects of the SIMS primary ion beam on the matrix crystal. There are a few possible ways to do this. The

voltage bias in the ToF-SIMS could be reversed so a negative potential may be applied. This would prevent electrons from bombarding the surface and causing local electric fields, which would presumably eliminate the surface damage. Another possible way of reducing surface damage is to sputter coat new crystals with ~ 1 nm of Au to increase surface conductivity. A coating this thin should allow ions to penetrate into the crystal surface, causing matrix molecule desorption. The craters could then be studied either in the AFM or the SEM, because surface charging would be reduced. This thin layer probably would not eliminate the high voltage damage because the surface would not be perfectly coated, but it would reduce surface deterioration in most areas enough to study the effects of the SIMS ion beam.

Further study should include a more in depth examination of surface damage due to the SIMS ion beam of a variety of standard MALDI matrices. It would be useful to test several common SIMS ions, ion energies, and fluences. The configuration that produces the deepest craters would likely be the most successful in ejecting large biomolecules, thus maximizing SIMS capabilities. To study surface damage more accurately, it may become necessary to develop a polishing procedure to achieve planar surfaces of the crystals before analysis.

References

- [1] K. J. Wu and R. W. Odom, *Anal. Chem.* **68**, 873 (1996).
- [2] A. Delcorte and B. J. Garrison, *J. Phys. Chem. B* **104**, 6785 (2000).
- [3] B. J. Garrison, A. Delcorte, and K. D. Krantzman, *Acc. Chem. Res.* **26**, 69 (2000).
- [4] J. Kampmeier, K. Dreisewerd, M. Schürenberg, and K. Strupat, *Int. J. Mass Spec.* **169/170**, 31 (1997).
- [5] A. M. Belu, D. J. Graham, and D. G. Castner, *Biomaterials.* **24**, 3635 (2003).
- [6] B. J. Garrison *et al.*, *App. Surf. Sci.* **203/204**, 69 (2003).
- [7] I. Fournier, C. Marinach, J. C. Tabet, and G. Bolbach, *J. Am. Soc. Mass Spec.* **14**, 893 (2003).
- [8] N. Winograd, *App. Surf. Sci.* **203/204**, 13 (2003).
- [9] “Atomic Force Microscope”. *Wikipedia*. 17 March 2005. 29 March 2005. <http://en.wikipedia.org/wiki/Atomic_Force_Microscope.>